Supplementary Information (SI) for Dalton Transactions.
This journal is © The Royal Society of Chemistry 2025

Supporting Information

Bis(formazanate) Iron(II) Complexes as Cathode Material for One-Compartment H_2O_2 Fuel Cell

Sunita Birara [a], *Moumita Majumder* [b], *Ramesh K. Metre**[a]

[a] Department of Chemistry, Indian Institute of Technology Jodhpur, Rajasthan- 342030, India

[b] Department of Chemistry, School of Science and Environmental Studies, Dr. Vishwanath Karad MIT World Peace University, Pune 411038, Maharashtra, India.

RECEIVED DATE (to be automatically inserted after your manuscript is accepted if required according to the journal that you are submitting your paper to)

CORRESPONDING AUTHOR FOOTNOTE: * To whom correspondence should be addressed. E-mail: rkmetre@iitj.ac.in Phone *(Office)*: (+91) 291-280-1309.

Table of Contents

Table S1. Crystal data and structure refinement for 1 and 2 (CCDC 2376420-2376421).

Identification code	1	2
Empirical formula	$C_{61}H_{38}Cl_2FeN_{10}S_2$	$C_{54}H_{34}Cl_2FeN_{10}O_2S_2$
Formula weight	1101.88	1045.78
Temperature/K	98(2)	98(2)
Crystal system	Triclinic	monoclinic
Space group	P-1	$P2_1/n$
a (Å)	12.155(3)	11.2395(4)
b (Å)	14.292(3)	31.2736(10)
c (Å)	16.758(4)	13.8511(5)
α (°)	114.981(5)	90
β (°)	97.046(6)	111.7710(10)
γ (°)	101.320(6)	90
Volume (Å^3)	2517.5(9)	4521.4(3)
Z	2	4
ρ_{calc}, g.cm^{-3}	1.454	1.536
μ (mm^{-1})	0.543	0.603
F(000)	1132.0	2144.0
Radiation	MoK_α (λ = 0.71073)	MoK_α (λ = 0.71073)
2Θ range for data collection (°)	5.3 to 56.746	4.782 to 56.72
Index ranges	$-16 \le h \le 16$, $-19 \le k \le 19$, $-22 \le l \le 22$	$-14 \le h \le 15$, $-41 \le k \le 41$, $-18 \le l \le 18$
Reflections collected	39556	73504
Independent reflections	12571 [R_{int} = 0.0454, R_{sigma} = 0.0487]	11259 [R_{int} = 0.0576, R_{sigma} = 0.0383]
Data/restraints/parameters	12571/0/685	11259/0/640
Goodness-of-fit on F^2	1.037	1.040
Final R indexes [I>=2σ (I)]	R_1 = 0.0724, wR_2 = 0.2009	R_1 = 0.0401, wR_2 = 0.0864
Final R indexes [all data]	R_1 = 0.0923, wR_2 = 0.2203	R_1 = 0.0566, wR_2 = 0.0964
Largest diff. peak/hole / (e Å^{-3})	1.17/-2.16	0.44/-0.52

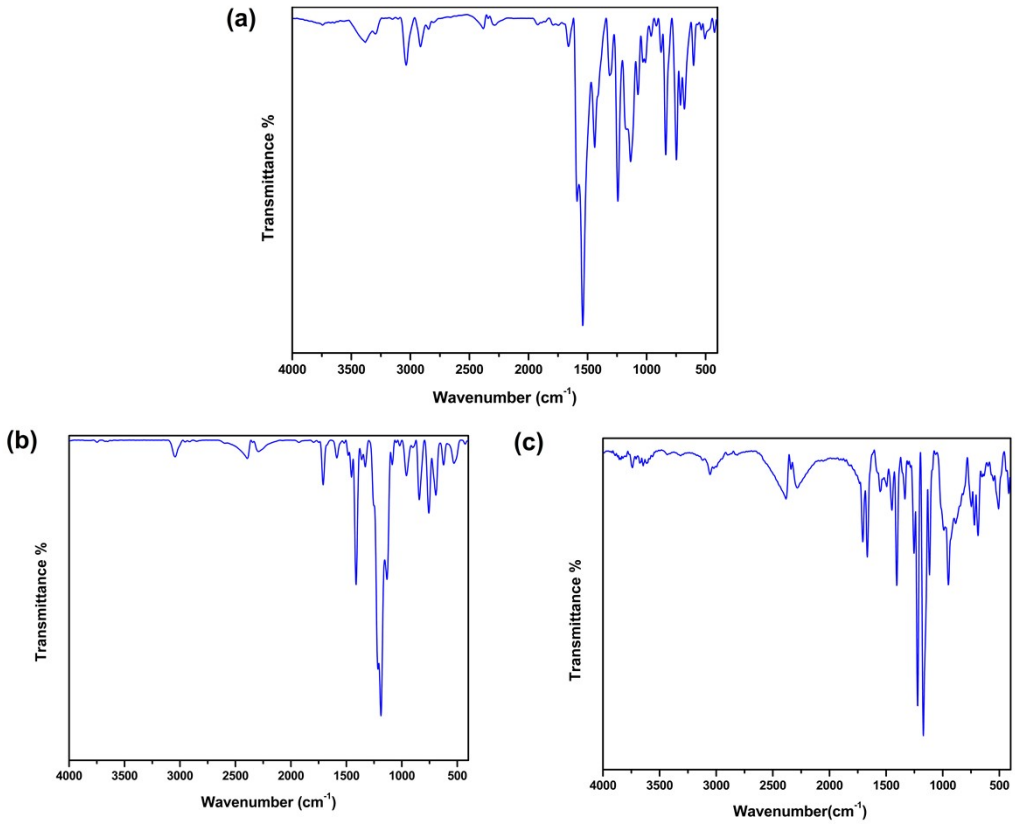

Fig S1. IR spectrum of (a) **L1H** (b) Complex **1** (c) Complex **2**.

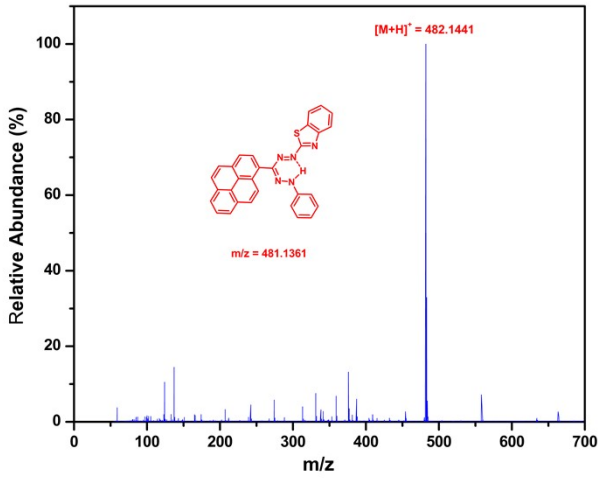

Figure S2. HRMS analysis for **L1H**: Anal. Calcd. for $[M+H]^+$ peak, m/z = 482.1361. Found $[M+H]^+$ peak, m/z = 482.1441.

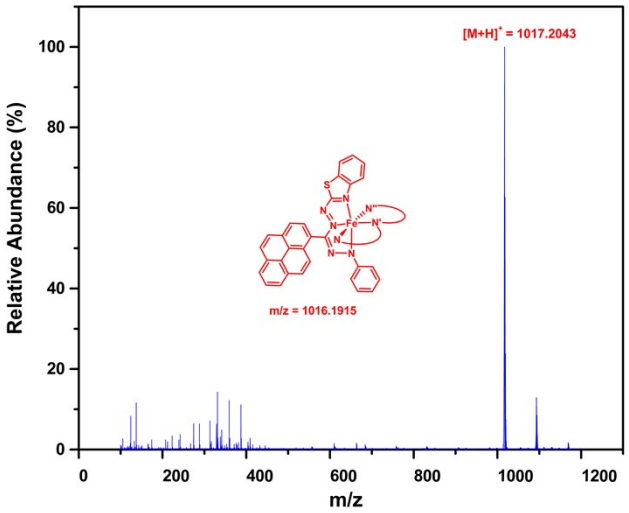

Figure S3. HRMS analysis for **1**: Anal. Calcd. for $[M+H]^+$ peak, m/z =1017.1915. Found $[M+H]^+$ peak, m/z = 1017.2043.

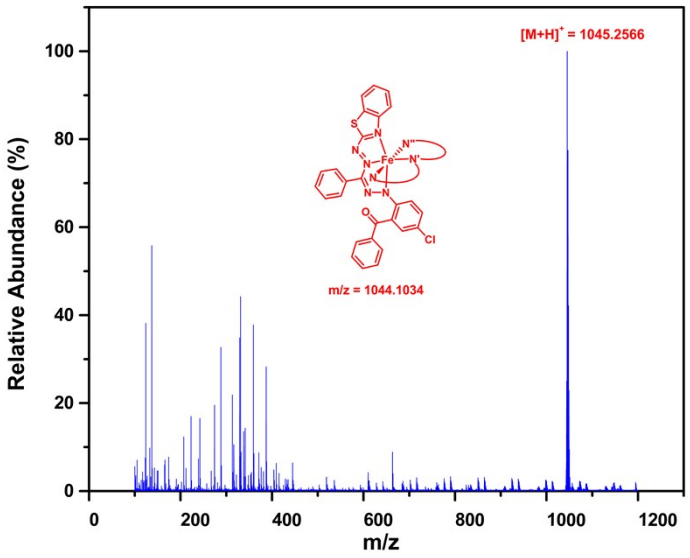

Figure S4. HRMS analysis for **2**: Anal. Calcd. for $[M+H]^+$ peak, m/z =1045.1034. Found $[M+H]^+$ peak, m/z = 1045.2566.

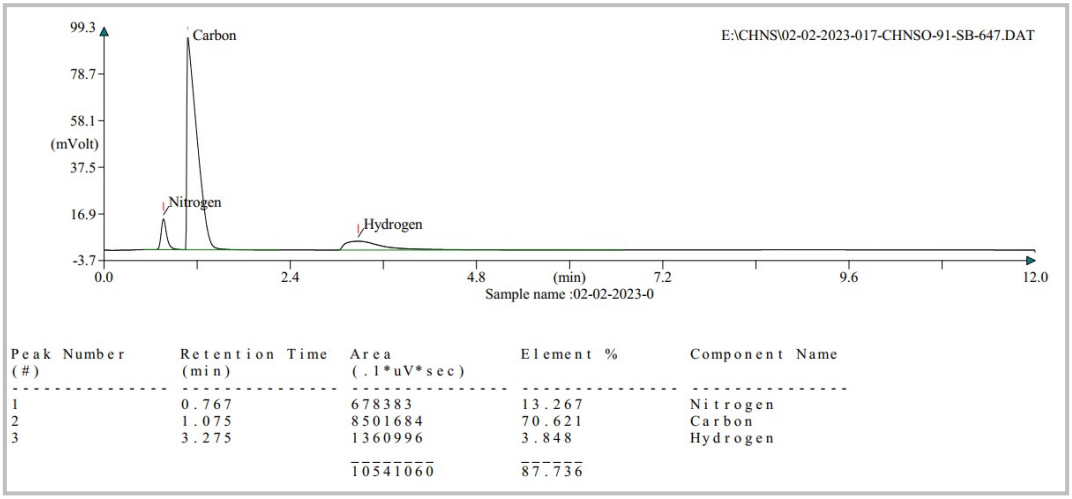

Peak Number (#)	Retention Time (min)	Area (.1*uV*sec)	Element %	Component Name
1	0.767	678383	13.267	Nitrogen
2	1.075	8501684	70.621	Carbon
3	3.275	1360996	3.848	Hydrogen
		10541060	87.736	

Figure S5. Elemental analysis of **1.** Anal. Calcd. (%) for $C_{60}H_{36}FeN_{10}S_2$: C, 70.86; H, 3.57; N, 13.77. Found: C, 70.62; H, 3.84; N, 13.26.

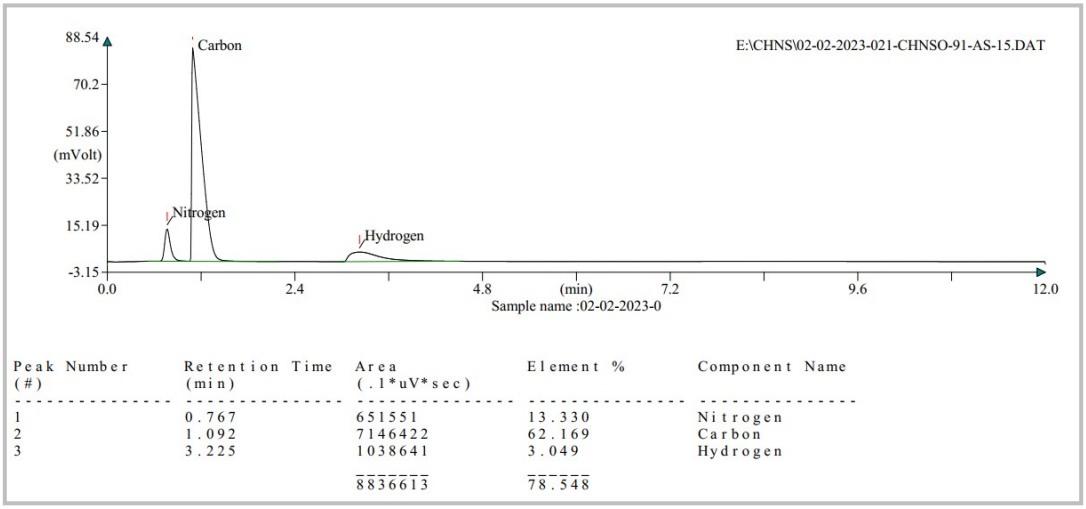

Peak Number (#)	Retention Time (min)	Area (.1*uV*sec)	Element %	Component Name
1	0.767	651551	13.330	Nitrogen
2	1.092	7146422	62.169	Carbon
3	3.225	1038641	3.049	Hydrogen
		8836613	78.548	

Figure S6. Elemental analysis of **2.** Anal. Calcd. (%) for $C_{54}H_{34}Cl_2FeN_{10}O_2S_2$: C, 62.02; H, 3.28; N, 13.39. Found: C, 62.169; H, 3.049; N, 13.330.

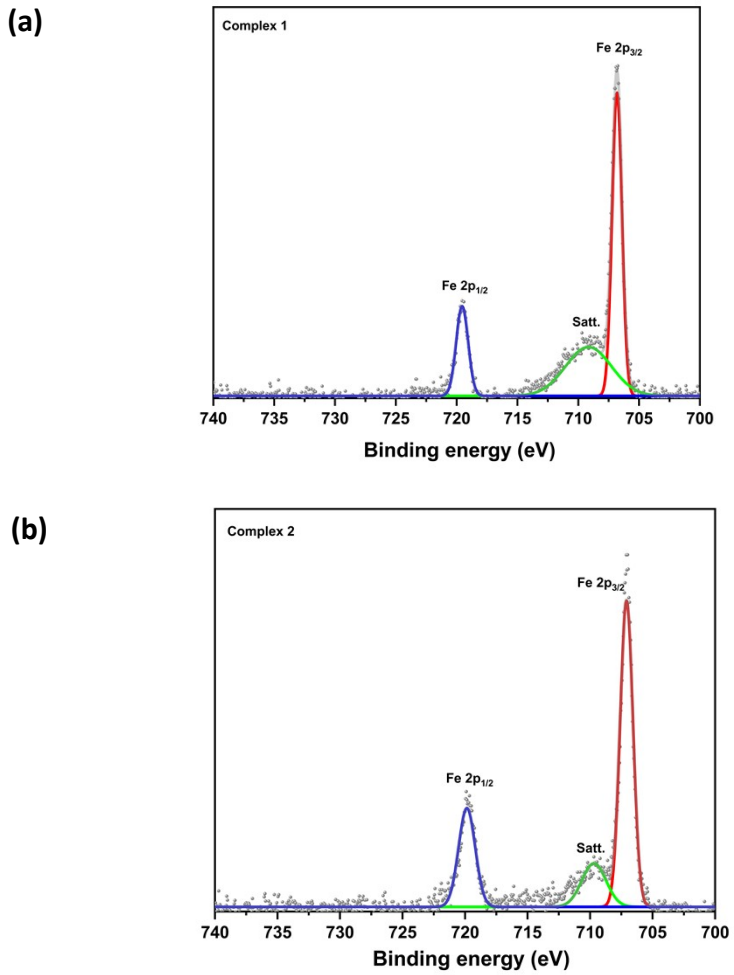

Figure S7. XPS-analysis for the Fe 2p binding energies of complexes (a) **1** and (b) **2**.

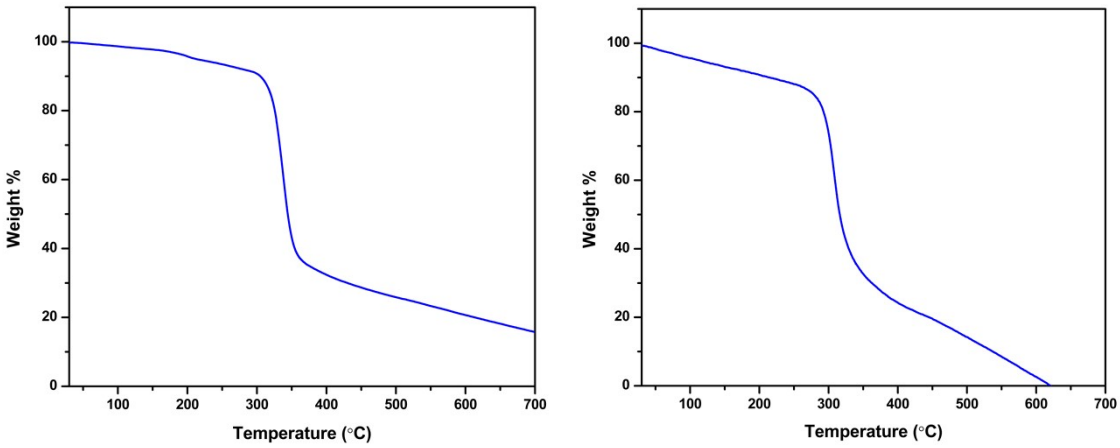

Figure S8. Thermogravimetric analysis of (left) complex **1**, (right) complex **2**.

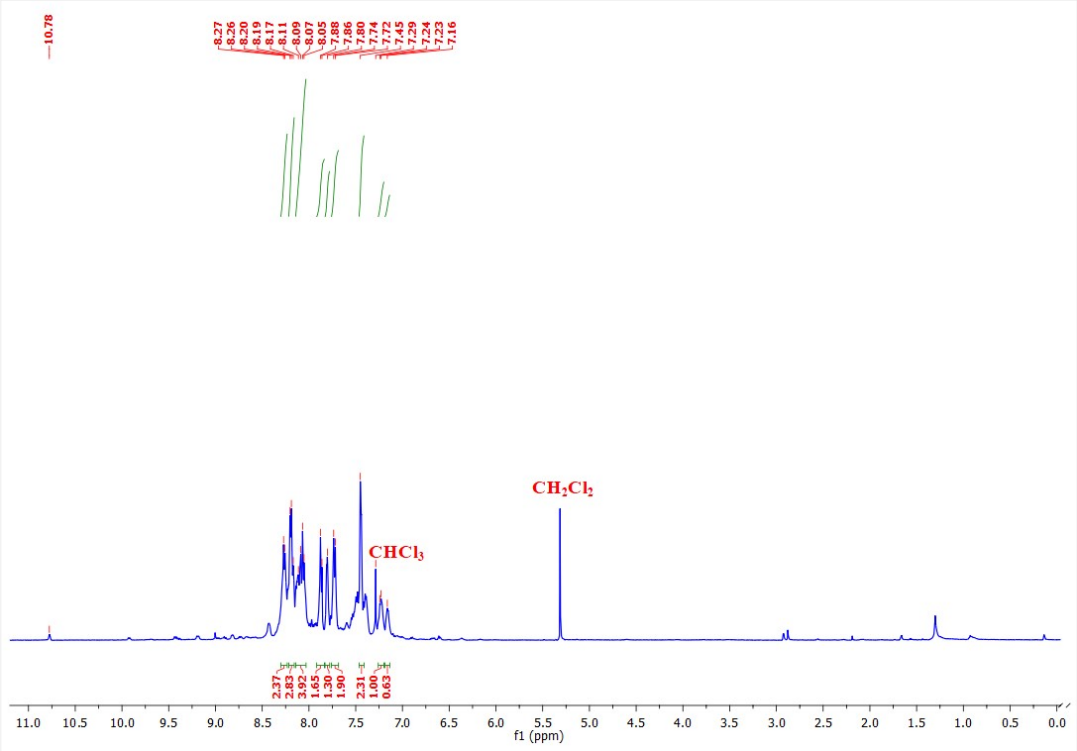

Figure S9. ^{1}H NMR of **L1H** in $CDCl_3$.

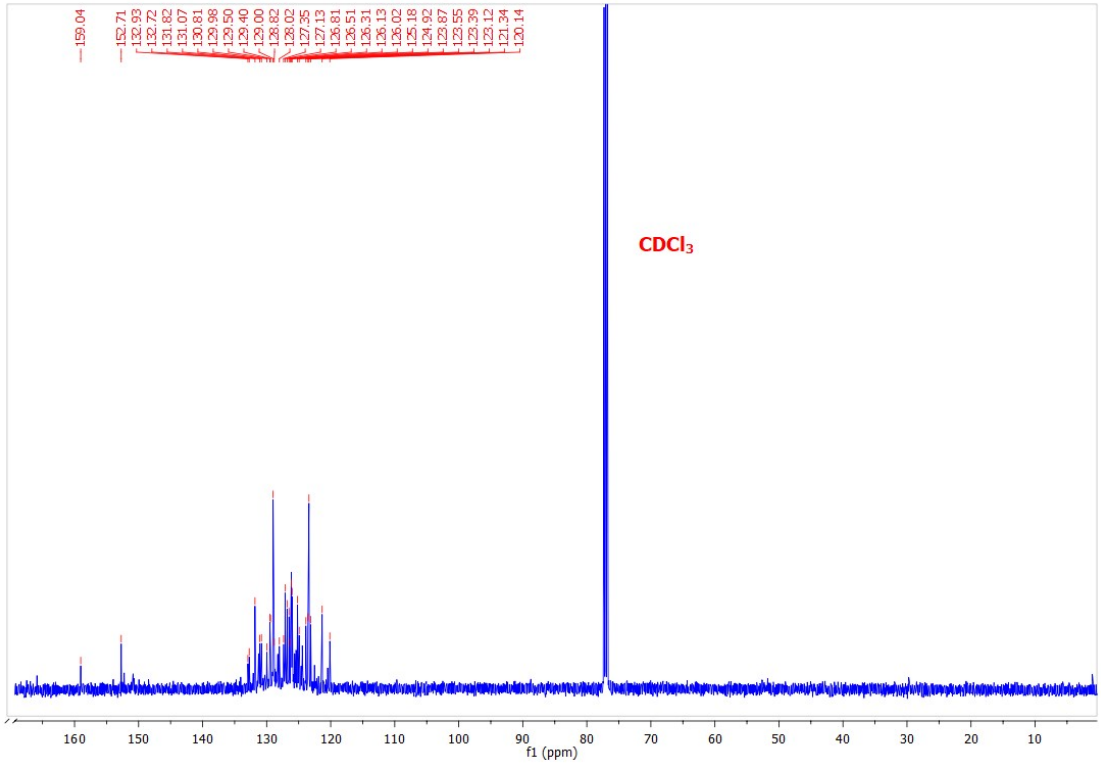

Figure S10. $^{13}C\{^{1}H\}$ NMR of **L1H** in $CDCl_3$.

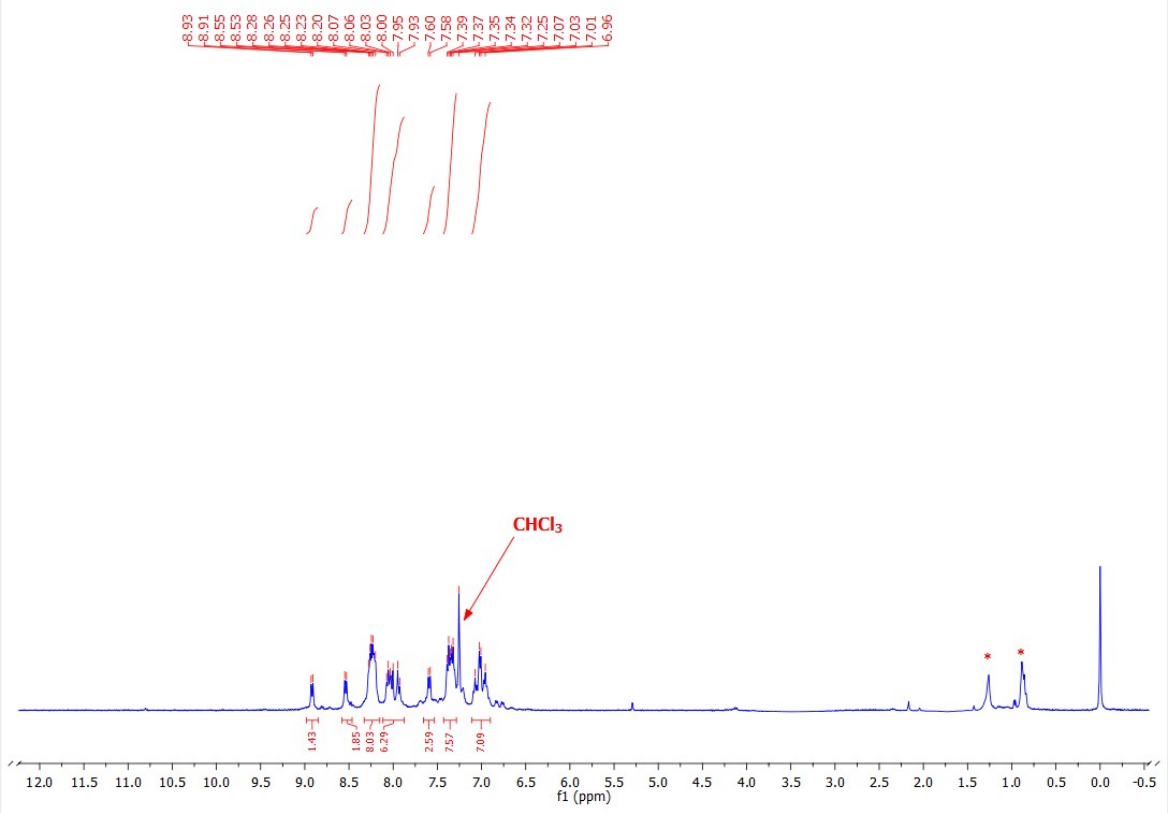

Figure S11. ^{1}H NMR of Complex **1** in $CDCl_3$.

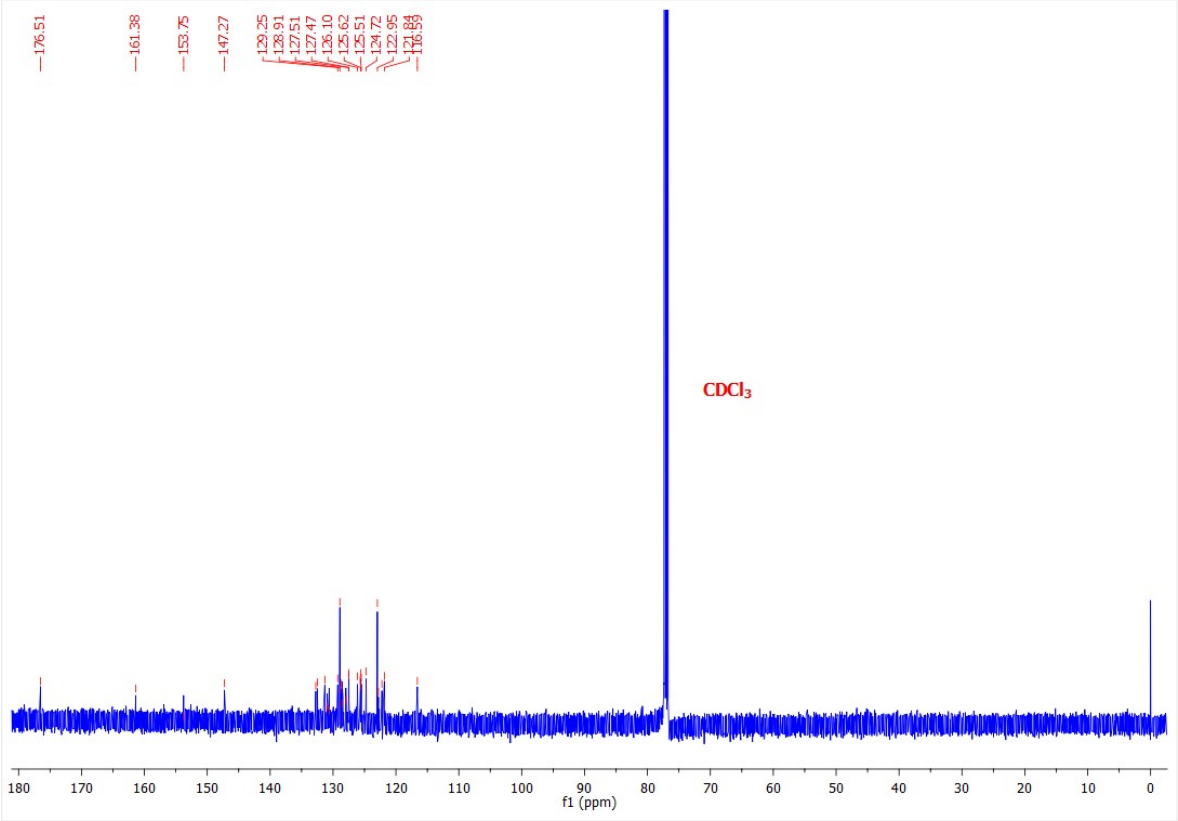

Figure S12. $^{13}C\{^{1}H\}$ NMR of complex **1** in $CDCl_3$.

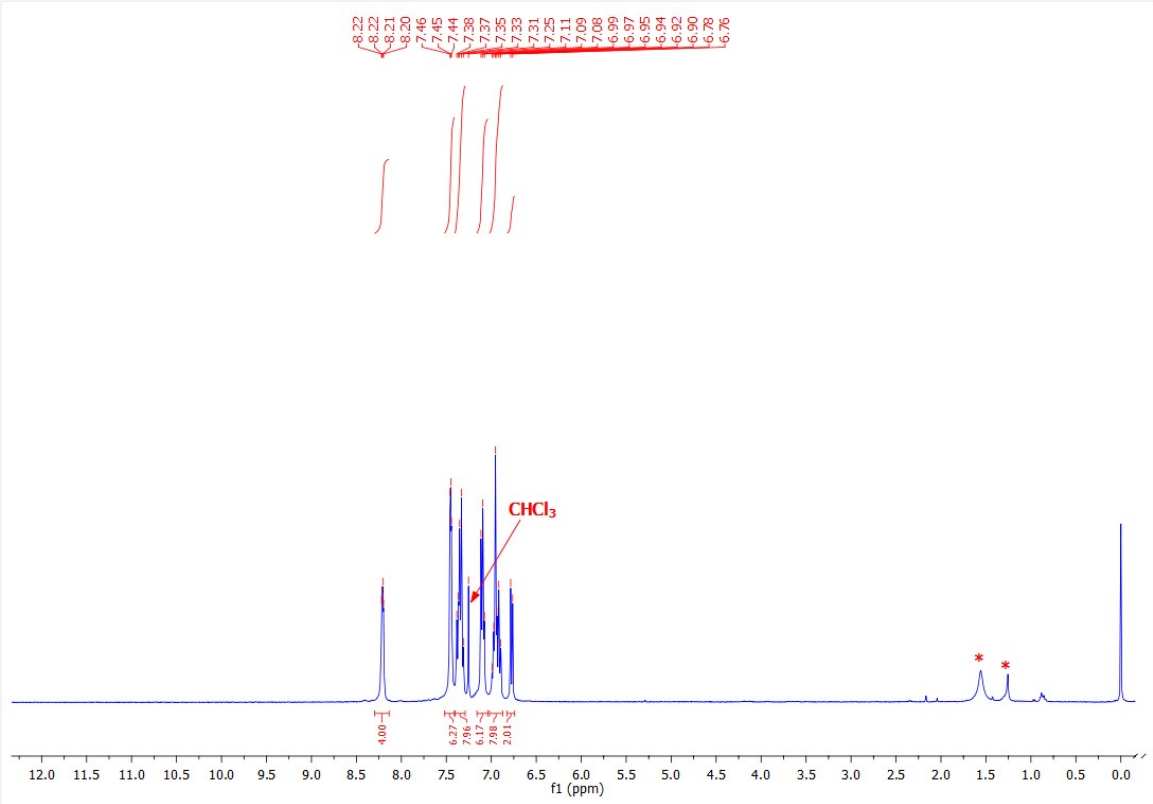

Figure S13. ^{1}H NMR of Complex **2** in $CDCl_3$.

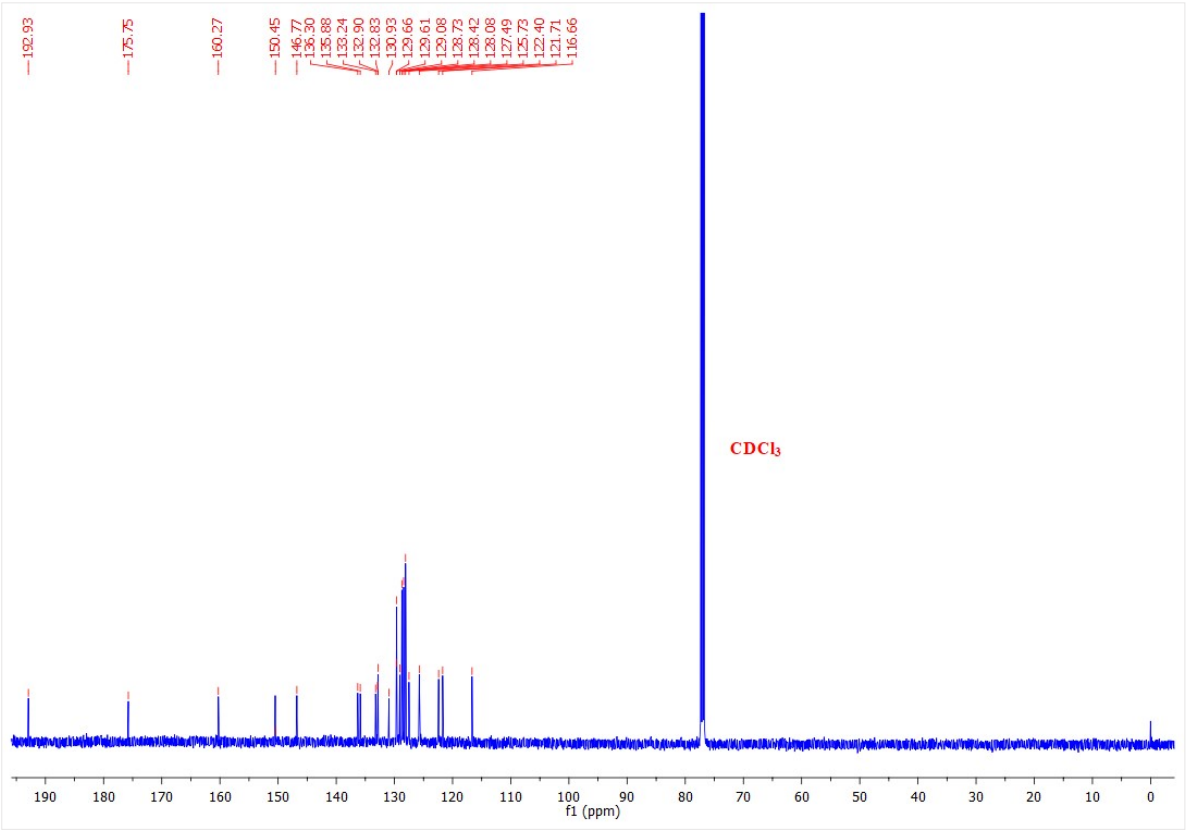

Figure S14. $^{13}C\{^{1}H\}$ NMR of complex **2** in $CDCl_3$.

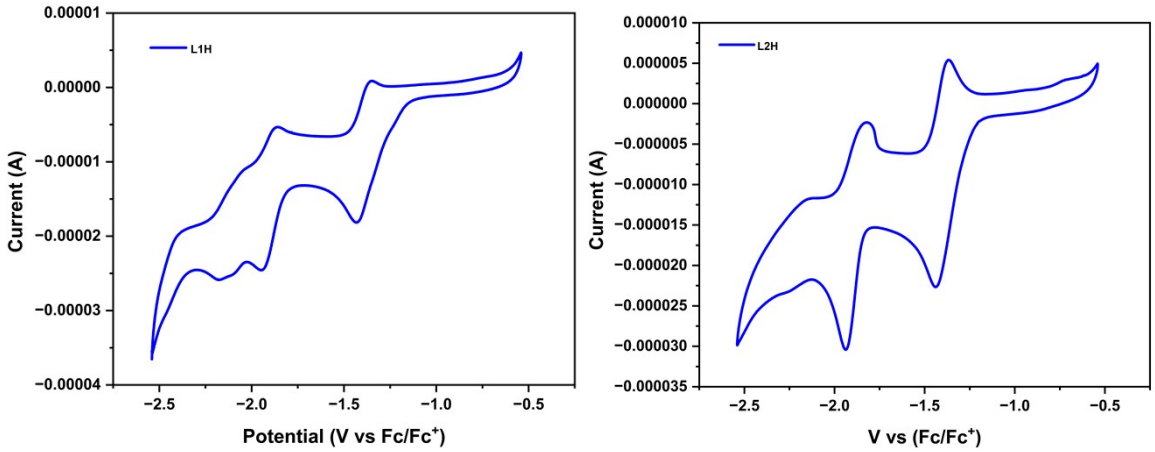

Figure S15. Cyclic voltammograms of complex (left) **L1H** and (right) **L2H** (1.5 mM solution of ligands in DMF; 0.1 M $[Bu_4N][PF_6]$ electrolyte; scan rate = 10 $mV \cdot s^{-1}$) acquired using a Pt working electrode, Pt-wire counter electrode, and Ag/AgCl (3.0 M KCl) reference electrode.

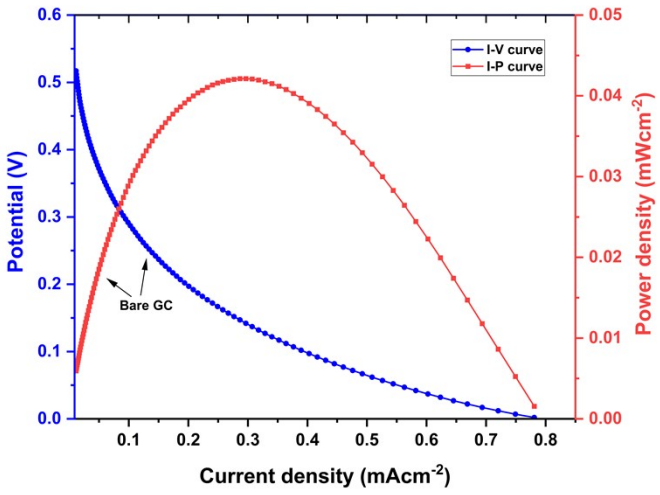

Figure S16. I–V(blue) and I–P (red) curves of a one-compartment H_2O_2 fuel cell with Ni anode and bare GC in 0.1 M HCl. Performance tests were conducted using 500 mM H_2O_2 with scan rate of 10mV s^{-1}. Currents and powers were normalized by the geometric surface area of an electrode.

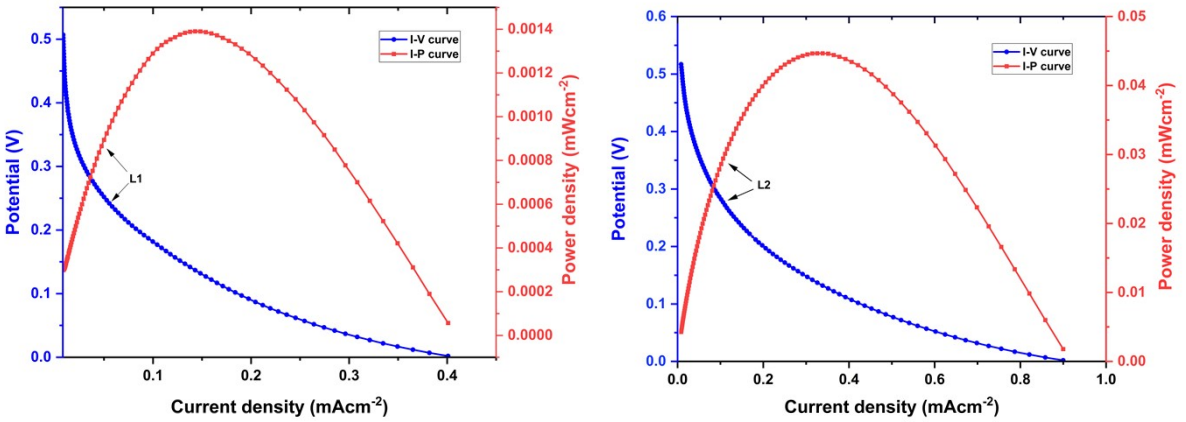

Figure S17. I–V(blue) and I–P (red) curves of a one-compartment H_2O_2 fuel cell with Ni anode and GC modified with (left) L1H and (right) L2H in 0.1 M HCl. Performance tests were conducted using 500 mM H_2O_2 with a scan rate of 10mV s^{-1}. Currents and powers were normalized by the geometric surface area of an electrode.

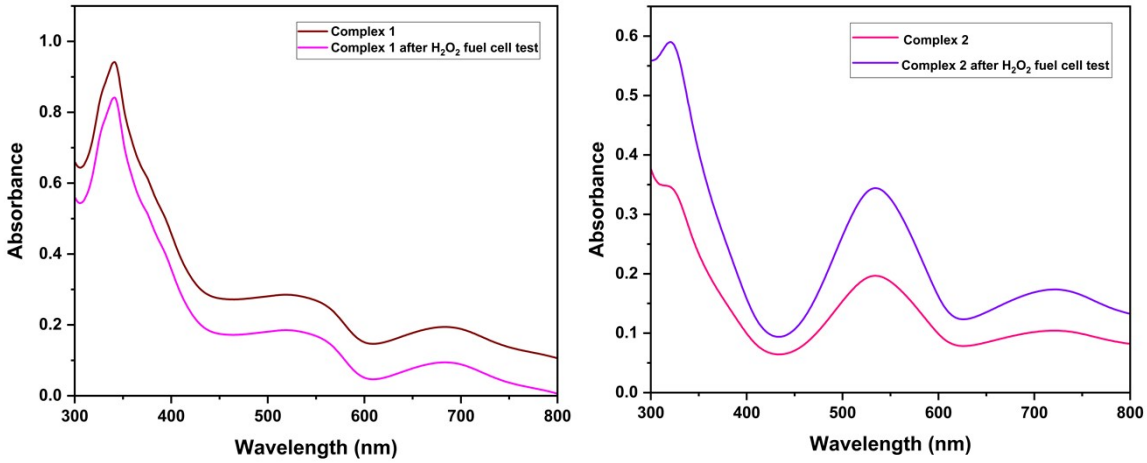

Figure S18. UV-vis spectra of (left) complex **1** and (right) complex **2** (blue line) and the recovered catalysts from the modified GC after running the H_2O_2 fuel cell test.

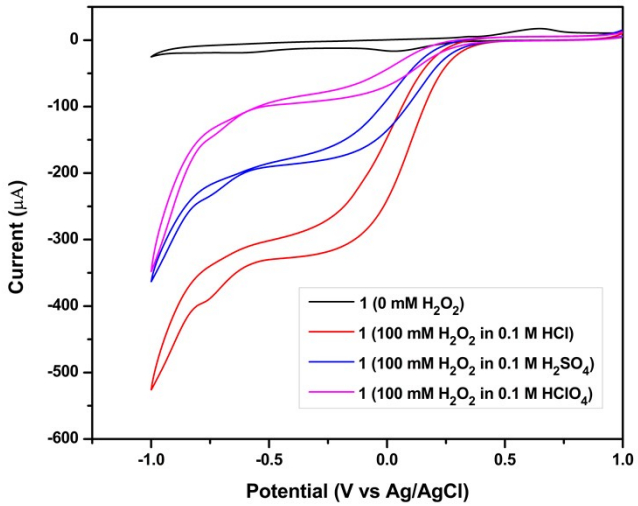

Figure S19. CV of H_2O_2 with **1** modified electrode in 0.1 M HCl (red line), 0.1 M H_2SO_4 (blue line) and 0.1M $HClO_4$ (pink line). CVs using modified Glassy Carbon electrode as working electrode in absence (black line) of H_2O_2 in acetate buffer (pH= 3) are also shown for reference. Ag/AgCl as reference and Pt-wire as counter electrode are used at a scan rate 50mV s^{-1}.

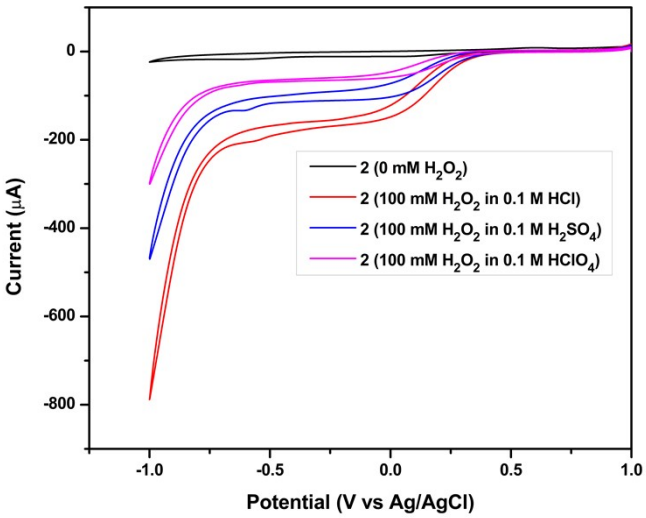

Figure S20. CV of H_2O_2 with **2** modified electrode in 0.1 M HCl (red line), 0.1 M H_2SO_4 (blue line) and 0.1M $HClO_4$ (pink line). CVs using modified Glassy Carbon electrode as working electrode in absence (black line) of H_2O_2 in acetate buffer (pH= 3) are also shown for reference. Ag/AgCl as reference and Pt-wire as counter electrode are used at a scan rate 50mV s^{-1}.

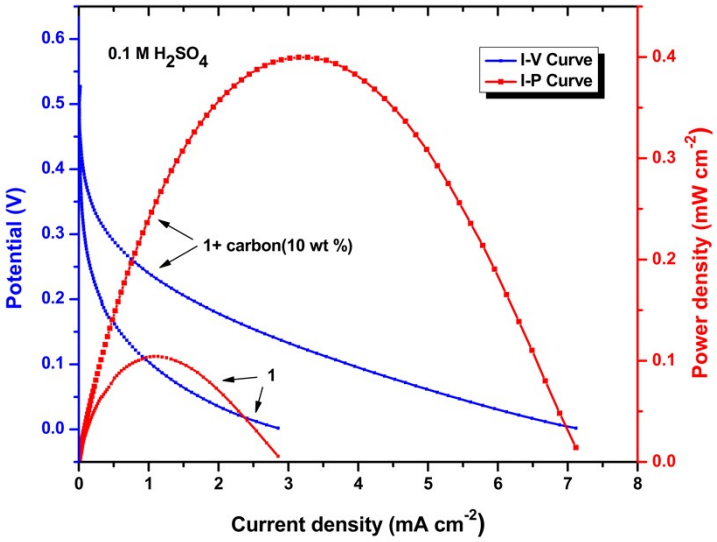

Figure S21. I–V(blue) and I–P (red) curves of a one-compartment H_2O_2 fuel cell with Ni anode and GC modified with **1** in 0.1 M H_2SO_4. Performance tests were conducted using 500 mM H_2O_2 with scan rate of 10mV s^{-1}. Currents and powers were normalized by the geometric surface area of an electrode.

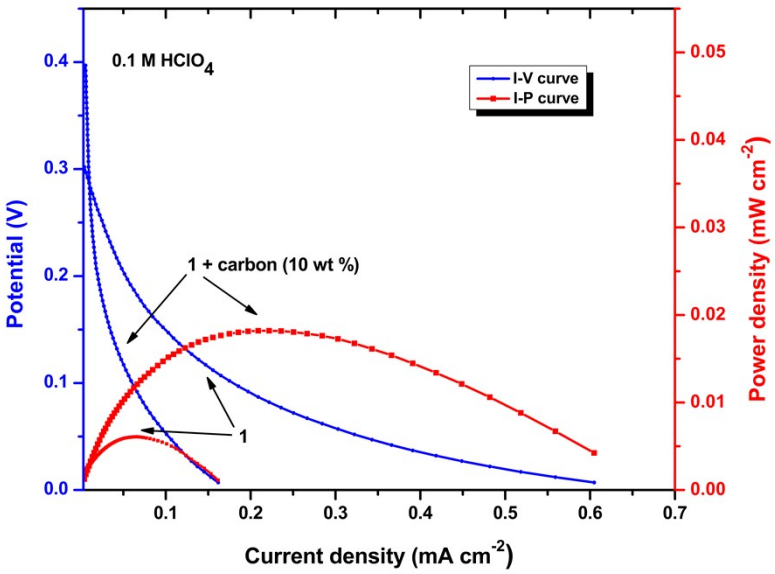

Figure S22. I–V(blue) and I–P (red) curves of a one-compartment H_2O_2 fuel cell with Ni anode and GC modified with **1** in 0.1 M $HClO_4$. Performance tests were conducted using 500 mM H_2O_2 with scan rate of 10mV s^{-1}. Currents and powers were normalized by the geometric surface area of an electrode.

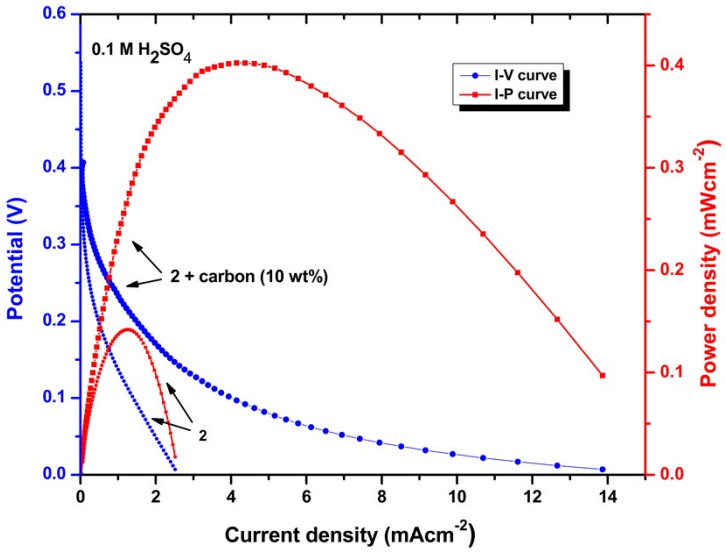

Figure S23. I–V(blue) and I–P (red) curves of a one-compartment H_2O_2 fuel cell with Ni anode and GC modified with **2** in 0.1 M H_2SO_4. Performance tests were conducted using 500 mM H_2O_2 with scan rate of 10mV s^{-1}. Currents and powers were normalized by the geometric surface area of an electrode.

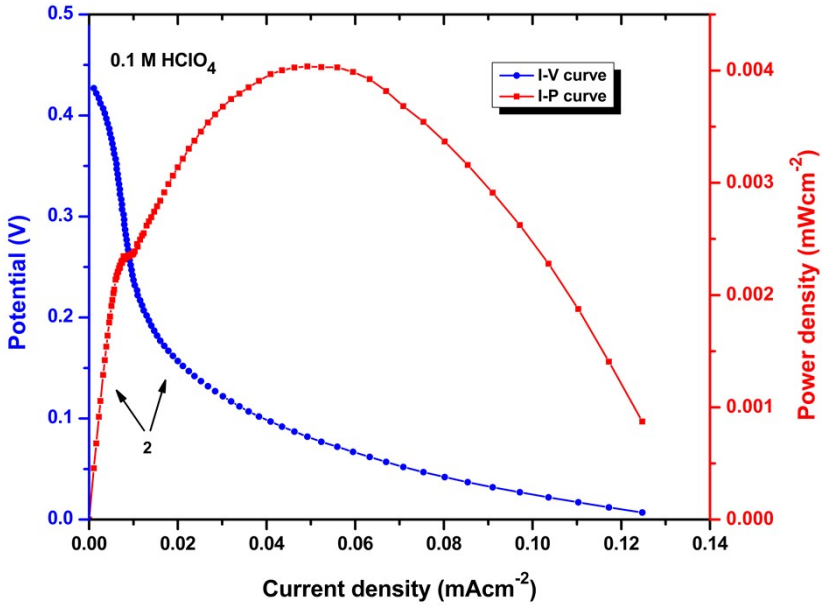

Figure S24. I–V(blue) and I–P (red) curves of a one-compartment H_2O_2 fuel cell with Ni anode and GC modified with **2** in 0.1 M $HClO_4$. Performance tests were conducted using 500 mM H_2O_2 with scan rate of 10mV s^{-1}. Currents and powers were normalized by the geometric surface area of an electrode.

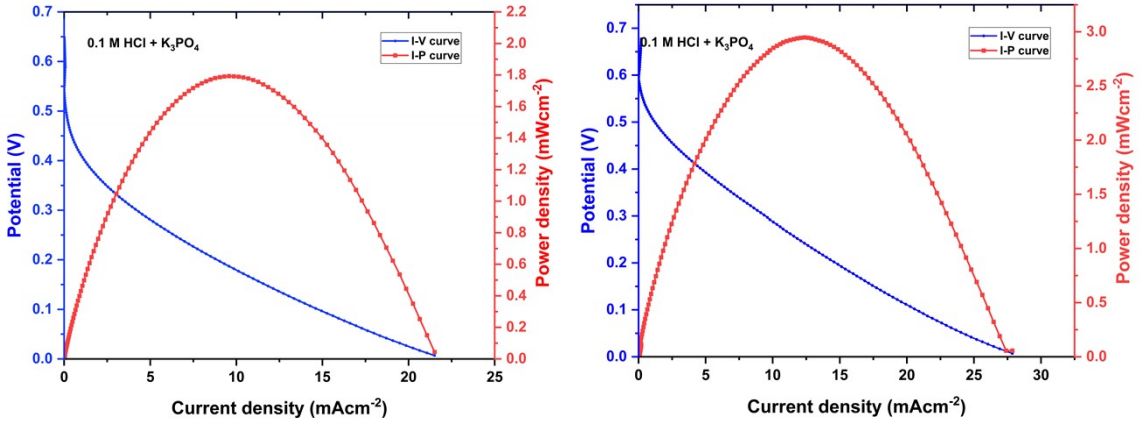

Figure S25. (Left) I–V(blue) and I–P (red) curves of a one-compartment H_2O_2 fuel cell with Ni anode and GC modified with **1** + 10 wt% C in 0.1 M HCl + K_3PO_4. (Right) I–V(blue) and I–P (red) curves of a one-compartment H_2O_2 fuel cell with Ni anode and GC modified with **2** + 10 wt% C in 0.1 M HCl + K_3PO_4.

Table S2: Comparison between the X-ray determined and DFT obtained a few selective geometric parameters of complex **1**.

S. no	X-Ray	DFT	
		B3LYP	BP86
Fe-N (S)	1.996/1.991	2.017/2.015	1.994/1.989
Fe-N(Bz)	1.933/1.942	1.974/1.978	1.935/1.939
Fe-N(Py)	1.884/1.884	1.898/1.896	1.877/1.878
N(S)-Fe-N(Bz)	156.24/157.01	157.55/157.21	158.03/157.57
N(Py)-Fe-N(Py)	177.73	177.83	177.38
N=N(S)	1.351/1.360	1.329/1330	1.347/1.344
N=N((Bz)	1.308/1.305	1.283/1.281	1.302/1.305
C-S-C	89.57/89.69	89.28/89.27	89.35/89.39

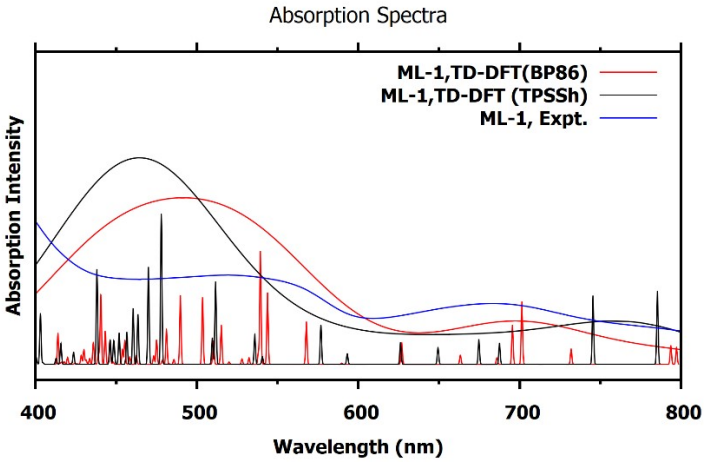

Figure S26. The computed absorption spectra obtained at unrestricted BP86 and TPSSh methods in conjugation with def2-TZVPP basis function. The spectrum obtained at BP86 method is found to be well accord with the experimental absorption spectra.

701 nm	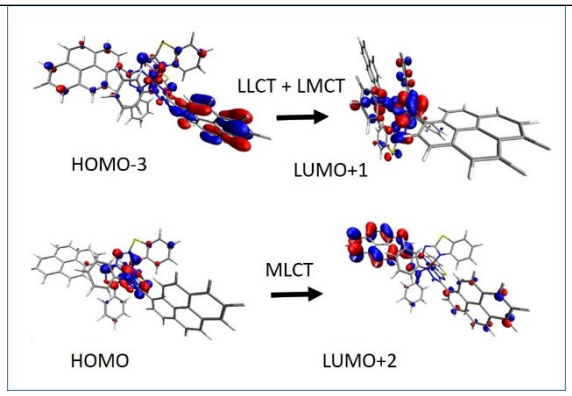
543 nm	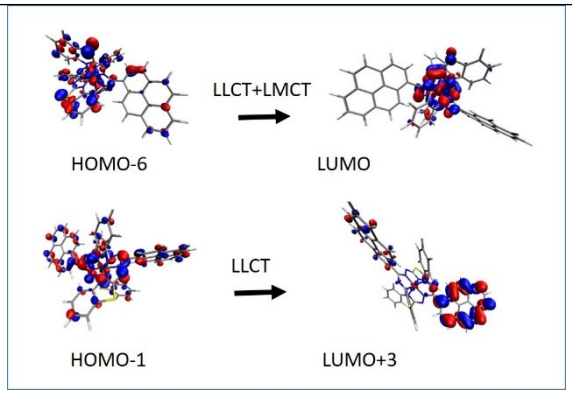

539 nm	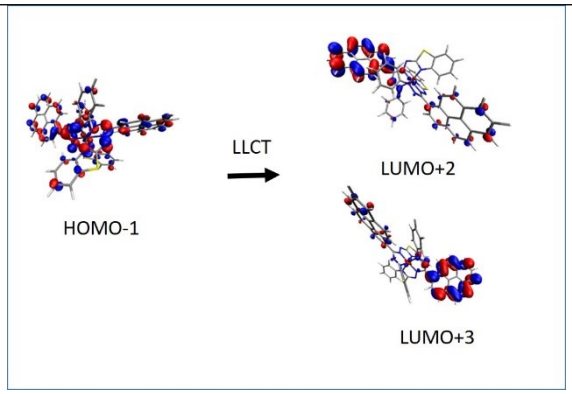

Figure S27. The molecular orbital representations of electronic transitions corresponding to the TD-DFT computed absorption spectrum of Complex 1 in $CHCl_3$ solvent in the wavelength range of 530-700 nm. A contour value of 0.03 au is used to generate the plots.